Fibroblast Growth Factor 21 Reverses Hepatic Steatosis, Increases Energy Expenditure, and Improves Insulin Sensitivity in Diet-Induced Obese Mice

Jing Xu,[1] David J. Lloyd,[1] Clarence Hale,[1] Shanaka Stanislaus,[1] Michelle Chen,[1] Glenn Sivits,[1] Steven Vonderfecht,[2] Randy Hecht,[3] Yue-Sheng Li,[3] Richard A. Lindberg,[1] Jin-Long Chen,[1] Dae Young Jung,[4] Zhiyou Zhang,[4] Hwi Jin Ko,[4] Jason K. Kim,[4] and Murielle M. Véniant[1]

OBJECTIVE—Fibroblast growth factor 21 (FGF21) has emerged as an important metabolic regulator of glucose and lipid metabolism. The aims of the current study are to evaluate the role of FGF21 in energy metabolism and to provide mechanistic insights into its glucose and lipid-lowering effects in a high-fat diet–induced obesity (DIO) model.

RESEARCH DESIGN AND METHODS—DIO or normal lean mice were treated with vehicle or recombinant murine FGF21. Metabolic parameters including body weight, glucose, and lipid levels were monitored, and hepatic gene expression was analyzed. Energy metabolism and insulin sensitivity were assessed using indirect calorimetry and hyperinsulinemic-euglycemic clamp techniques.

RESULTS—FGF21 dose dependently reduced body weight and whole-body fat mass in DIO mice due to marked increases in total energy expenditure and physical activity levels. FGF21 also reduced blood glucose, insulin, and lipid levels and reversed hepatic steatosis. The profound reduction of hepatic triglyceride levels was associated with FGF21 inhibition of nuclear sterol regulatory element binding protein-1 and the expression of a wide array of genes involved in fatty acid and triglyceride synthesis. FGF21 also dramatically improved hepatic and peripheral insulin sensitivity in both lean and DIO mice independently of reduction in body weight and adiposity.

CONCLUSIONS—FGF21 corrects multiple metabolic disorders in DIO mice and has the potential to become a powerful therapeutic to treat hepatic steatosis, obesity, and type 2 diabetes. ***Diabetes*** **58:250–259, 2009**

Fibroblast growth factor (FGF) 21 is a member of the FGF superfamily (1). It is most closely related to FGF19 and FGF23, sharing ~30–35% amino acid sequence homology (1). The FGF19 subfamily comprises FGF19, FGF21, and FGF23 (2), and all three FGF19 subfamily members have recently emerged as metabolic hormones involved in the regulation of glucose, lipid, bile acid, and phosphate metabolism (2–6).

FGF21 was isolated from a mouse embryo cDNA library and appeared as an atypical FGF preferentially expressed in tissues related with metabolic functions, such as liver (7) and pancreas (J.X., S. Sheila, unpublished data). A biological activity of FGF21 was revealed in a high-throughput assay looking for secreted proteins that stimulate glucose uptake in 3T3-L1 adipocytes (5). Further studies demonstrated that FGF21 increased the expression of GLUT1 and stimulated GLUT1-mediated glucose uptake in differentiated adipocytes (5). When recombinant FGF21 protein was administered to *ob/ob* and *db/db* mice and Zucker fatty rats, which are rodent models of diabetes, it lowered blood glucose and triglycerides to near-normal levels (5). In diabetic rhesus monkeys, treatment also resulted in a favorable lipoprotein profile, which included reduced LDL cholesterol and increased HDL cholesterol (8). Furthermore, transgenic mice with hepatic overexpression of FGF21 were lean and protected from high-fat diet–induced insulin resistance (5,9).

Recent progress has also been made in elucidating the receptor signaling complex and cellular functions of FGF21. In vitro studies suggest that FGF21 initiates its action by activating a unique dual receptor complex consisting of a coreceptor β-klotho and the tyrosine kinase FGF receptors (FGFRs) (10–12). β-klotho binds FGF21 and facilitates its activation of FGFRs (11,12). β-klotho is predominantly expressed in metabolic organs, including liver, adipose tissue, and pancreas (13), and may define the in vivo sites where FGF21 acts. FGF21 has been shown to stimulate glucose uptake in adipocytes (5) and to inhibit glucagon secretion and preserve insulin content in pancreatic islets (5,14). Additionally, FGF21 has also been shown to enhance hepatic lipid oxidation and ketone body production (9,15).

The metabolic effects of FGF21 have been previously evaluated by other groups using monogenic leptin-deficient and age-related spontaneous insulin-resistant models (5,8). We conducted our studies using a high-fat diet–induced obesity (DIO) model, because the metabolic characteristics of DIO more closely resemble those of human type 2 diabetes and could therefore provide a broader measure of the various associated metabolic parameters. In this report, our objective was to evaluate the role of FGF21 in energy metabolism and to provide mechanistic insights into its underlying glucose and lipid-lowering effects.

From the [1]Department of Metabolic Disorders, Amgen, Thousand Oaks, California; the [2]Department of Pathology, Amgen, Thousand Oaks, California; the [3]Department of Protein Sciences, Amgen, Thousand Oaks, California; and the [4]Department of Cellular and Molecular Physiology, Pennsylvania State University College of Medicine, Hershey, Pennsylvania.

Corresponding author: Jing Xu, jingx@amgen.com.

Received 19 March 2008 and accepted 29 September 2008.

Published ahead of print at http://diabetes.diabetesjournals.org on 7 October 2008. DOI: 10.2337/db08-0392.

RESEARCH DESIGN AND METHODS

Preparation of recombinant FGF21. Recombinant murine FGF21 (amino acids 30–210) was expressed in *Escherichia coli*. It was folded in solubilized inclusion bodies and purified by ion exchange and hydrophobic interaction chromatography to obtain >90% purity.

Animals and treatments. Male C57BL/6 mice were obtained from Charles Rivers Laboratories (Wilmington, MA) at 3 weeks of age. After 12 weeks of a diet period, either a standard diet (8640; Harlan Teklad, Indianapolis, IN) or a high-fat diet (D12492, Research Diets, New Brunswick, NJ), mice were randomly assigned to treatment or vehicle groups, and the randomization was stratified by body weight and fed blood glucose levels. The mice were intraperitonally injected with vehicle or FGF21 twice daily (at one-half of the daily dose) to achieve the indicated daily dose for each of the experiments performed. Mice were maintained on their respective diets during the drug treatment periods. All experiments were approved by the Institutional Animal Care and Use Committee (IACUC) at Amgen.

Metabolic effects. In a 6-week pharmacological study, FGF21 was administrated to DIO mice at 0 (vehicle), 0.1, 1, and 10 mg · kg^{-1} · day^{-1}. A group of DIO mice was treated with rosiglitazone formulated in the high-fat diet at 50 mg/kg diet to provide a dose of ~4 mg · kg^{-1} · day^{-1}. Body weight was recorded every other day, and food intake was measured every 6 days throughout the study. At day 24, blood was collected from the retro-orbital sinus of each nonanesthetized mouse to measure blood glucose, insulin, glucagon, leptin, triglyceride, cholesterol, free fatty acids, aspartate aminotransaminase (AST), alanine aminotransaminase (ALT), and alkaline phosphatase (ALP) levels. Body composition was analyzed on day 27 using an EchoMRI-100 analyzer (Echo Medical Systems, Houston, TX). A glucose tolerance test (GTT) was performed on day 30 with an intraperitonal injection of a 2 mg/kg glucose solution after a 12-h fast. Terminal decapitated trunk blood was collected to measure β-hydroxybutyrate. Tissues were collected for lipid analysis, mRNA and protein expression analysis, and histological examinations.

Analysis of endocrine hormones and metabolites. Plasma insulin, glucagon, and leptin were measured with a mouse endocrine multiplex assay (Linco Research, St. Charles, MO). Blood glucose was measured with a OneTouch Glucometer (LifeScan, Milpitas, CA). Plasma cholesterol, triglyceride, nonesterified fatty acids, AST, ALT, and ALP were measured using an Olympus AU400e Chemistry Analyzer (Olympus America, Center Valley, PA). Plasma β-hydroxybutyrate concentration was measured using D-3-hydroxybutyric acid colorimetric method (R-Biopharm, Marshall, MI). Hepatic and muscle lipid extraction was conducted as described previously (16,17), and lipid contents were measured with a triglyceride kit (TR0100; Sigma-Aldrich, St. Louis, MO) and a cholesterol kit (Boehringer Mannheim, Ridgefield, CT).

Quantitative real-time PCR and Western analysis. RNA was isolated from liver samples using the RNeasy kit (Qiagen, Valencia, CA). The reactions were carried out with 100 ng total RNA using TaqMan One Step PCR kit with 6-carboxy-fluorescein (FAM) dye-labeled TaqMan chemistry (Applied Biosystems, Foster City, CA). Cyclophilin A was used as the internal standard. Relative gene expression was analyzed using an ABI 7900 sequence detection system. Western blot analyses were performed using total protein extracted from frozen liver samples using radioimmunoprecipitation assay lysis buffer containing protease inhibitors. The following primary antibodies were used: monoclonal anti–sterol regulatory element binding protein-1 (anti-SREBP1; IgG-2A4) prepared from hybridoma cells (CRL 2121; American Type Culture Collection); rabbit polyclonal anti–peroxisome proliferator–activated receptor γ (anti-PPARγ) (2435; Cell Signaling); monoclonal anti–fatty acid synthase (anti-FAS) antibody (610962; BD Biosciences); and monoclonal anti–β-actin (ACTB12-M; Alpha Diagnostic). Total acetyl-CoA carboxylase (ACC) was probed with streptavidin-horseradish peroxidase (E34; Biomeda) as described previously (18).

Histology. Tissues were fixed in 10% zinc-formalin. Tissues were processed, embedded in paraffin, sectioned at a thickness of 5 μm, and stained with hematoxylin-eosin (H-E). For oil-red-O staining, livers were snap-frozen in isopentane cooled in liquid nitrogen, embedded in optimum cutting temperature, and sectioned on a cryostat.

Indirect calorimetry. Recombinant FGF21 was administered to DIO mice at 1 and 10 mg · kg^{-1} · day^{-1} divided into two daily injections for a period of 19 days. Metabolic rate was assessed using the Comprehensive Laboratory Animal Monitoring System (Columbus Instruments, Columbus, OH). Data on O_2 consumption (Vo_2; milliliters per hour per mouse), CO_2 production (Vco_2; milliliters per hour per mouse), and activity (beam breaks) were collected every 20 min for the entire 19 days. Respiratory quotient was derived from the ratio of Vo_2 to Vco_2, and energy expenditure was calculated as follows: Energy expenditure = (3.815 + 1.232 × respiratory quotient) × Vo_2. Daily body weight and food intake were manually measured.

Hyperinsulinemic-euglycemic clamp. This study was performed at the Pennsylvania State Diabetes & Obesity Mouse Phenotyping Center and approved by Pennsylvania State University IACUC. Briefly, mice were fed standard diet or high-fat diet for 15 weeks and treated with FGF21 or vehicle during the last 3 weeks of the diet period. One group of mice fed standard diet was administered a 10 mg · kg^{-1} · day^{-1} dose of FGF21, and two groups of DIO mice were administered 0.1 and 10 mg · kg^{-1} · day^{-1} doses of FGF21. After an overnight fast, a 2-h hyperinsulinemic-euglycemic clamp was conducted as previously described (19). Basal and insulin-stimulated whole-body glucose turnover were estimated using a continuous infusion of [3-^{3}H]glucose (PerkinElmer, Boston, MA) for 2 h before the clamps (0.05 μCi/min) and throughout the clamps (0.1 μCi/min), respectively. Whole-body glycogen plus lipid synthesis is calculated as the difference between whole-body glucose turnover and glycolysis. To estimate insulin-stimulated glucose uptake in individual tissues, 2-deoxy-D-[1-^{14}C]glucose (2-[^{14}C]DG; PerkinElmer) was administered (10 μCi) 75 min after the start of the clamps. Blood samples were taken before, during, and at the end of clamps for measurement of plasma [^{3}H]glucose, ^3H_2O, 2-[^{14}C]DG concentrations, and/or insulin concentrations. At the end of the clamp, tissues (gastrocnemius, tibialis anterior, quadriceps, white and brown adipose, liver, and heart) were taken for biochemical analysis as previously described (19).

Statistical analysis. Data are presented as means ± SE. Statistical comparison of the means among the groups was made using one-way ANOVA. Differences between the means of individual groups were analyzed by the post hoc Fisher's test using Statview software (SAS Institute, Cary, NC).

RESULTS

Recombinant FGF21 reduces body weight and adiposity. Figure 1*A* shows representative mice fed either standard diet or high-fat diet treated with vehicle, 10 mg · kg^{-1} · day^{-1} FGF21, or rosiglitazone (~4 mg · kg^{-1} · day^{-1}) for 6 weeks. Compared with age-matched mice on standard diet, mice on high-fat diet were markedly heavier with elevated body fat mass (Fig. 1*A–C*). Treatment with FGF21 (1 and 10 mg · kg^{-1} · day^{-1}) reduced body weight by 8 and 22% at the end of 6 weeks of study (Fig. 1*B*) and was associated with 15 and 36% reductions in body fat mass, respectively (Fig. 1*C*). Marginal but statistically significant decreases in lean mass were also observed based on body composition analysis (Fig. 1*C*). Throughout the treatment period, DIO mice treated with the lowest dose of FGF21 (0.1 mg · kg^{-1} · day^{-1}) had relatively stable body weights (Fig. 1*B*), which were not significantly different from those of vehicle-treated DIO mice (6 vs. 8% body weight gain from baseline, 50.2 ± 0.7 vs. 51.4 ± 0.9 g at the end of study; treated vs. vehicle). FGF21 treatment did not reduce the amount of daily food intake in DIO mice (Fig. 1*D*). Considering the reduced body weight, mice treated with FGF21 appeared hyperphagic.

Recombinant FGF21 improves glucose and lipid homeostasis. Administration of FGF21 resulted in a dose-dependent reduction in circulating levels of glucose, insulin, cholesterol, triglycerides, free fatty acids, and leptin (Fig. 2*A–E*). There were no significant changes in plasma glucagon levels (Table 1). Plasma β-hydroxybutyrate was statistically significantly reduced after 6 weeks of FGF21 treatment (1 and 10 mg · kg^{-1} · day^{-1}) (Table 1). A GTT was performed on study day 30 (Fig. 2*F*) after a 12-h fast. At time 0, the fasting blood glucose levels of FGF21-treated DIO mice were significantly lower than those of vehicle-treated DIO mice and approached levels typically found in normal lean mice. The glucose excursions after the glucose challenge were dose dependently improved by FGF21 treatment. It is worth noting that the lowest dose (0.1 mg · kg^{-1} · day^{-1}) of FGF21 reduced plasma glucose, insulin, and lipid levels (Fig. 2*A–D*) and restored glucose tolerance as effectively as rosiglitazone (Fig. 2*F*) in the absence of reduction in body weight (Fig. 1*B*), body fat content (Fig. 1*C*), or plasma leptin (Fig. 2*E*) levels.

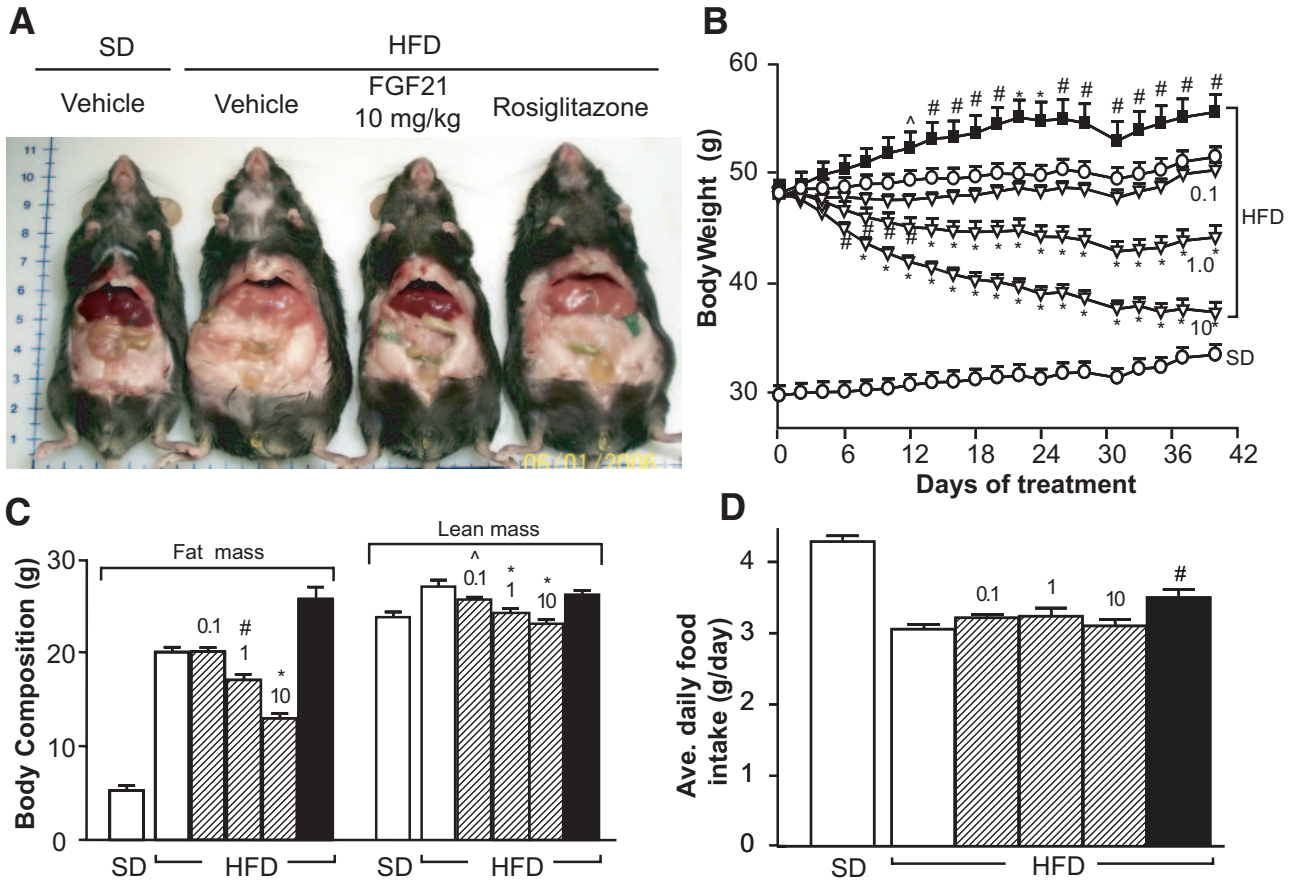

FIG. 1. Reversal of high-fat diet–induced obesity by recombinant FGF21 in DIO mice. DIO mice were treated with recombinant murine FGF21 intraperitonally at doses of 0 (vehicle), 0.1, 1, or 10 mg · kg^{-1} · day^{-1} divided into two daily injections. An additional group of DIO mice was treated with rosiglitazone formulated in the high-fat diet to provide a dose of ~4 mg · kg^{-1} · day^{-1}. Mice on standard diet (SD) were included as controls and injected intraperitonally with vehicle. *A*: Photograph of representative mice either fed standard diet and administered vehicle or fed high-fat diet and administered vehicle, 10 mg · kg^{-1} · day^{-1} FGF21, or rosiglitazone for 6 weeks. *B*: Body weight monitored throughout the treatment. *C*: Body composition analyzed after 27 days of treatment. *D*: Average daily food intake during 6 weeks of treatment. Vehicle (open circles or open bars); FGF21 (open triangles or striped bars; 0.1, 1, and 10 denote FGF21 doses in mg · kg^{-1} · day^{-1}); rosiglitazone (black squares or black bars). All data are means ± SE, n = 10 per group, $\wedge P < 0.05$; #$P < 0.01$; *$P < 0.001$ vs. vehicle-treated high-fat diet mice. (Please see http://dx.doi.org/10.2337/db08-0392 for a high-quality digital representation of this figure.)

Recombinant FGF21 reverses hepatic steatosis and decreases tissue lipid contents in DIO mice. Histological examination of liver sections stained with H-E (Fig. 3*A–D*) and oil-red-O (Fig. 3*E–H*) showed that there was extensive micro- and macrovesicular hepatocyte vacuolation (Fig. 3*B*), reflecting intrahepatic fat accumulation (Fig. 3*F*) in vehicle-treated DIO mice. In contrast, hepatocellular vacuolation and intense oil-red-O–stained lipid droplets were not observed in liver sections from FGF21-treated DIO mice (Fig. 3*C* and *G*). Biochemical analysis showed marked reductions of hepatic triglyceride and cholesterol content (Table 1) in livers of FGF21-treated DIO mice, accompanied by reductions of plasma AST, ALT, and ALP levels (Table 1). Treatment with rosiglitazone did not improve the steatotic state (Fig. 3*D* and *H*; Table 1). Muscle triglyceride content was decreased in DIO mice treated with 10 mg/kg FGF21 (Table 1). Muscle cholesterol content was also reduced after FGF21 treatment; however, this reduction was not statistically significant (Table 1). Histological examination of brown adipose tissue sections (Fig. 3*I–L*) also showed reduced lipid accumulation in FGF21-treated DIO mice (Fig. 3*K*) compared with vehicle-treated mice (Fig. 3*J*). No significant histological changes were observed with respect to the pancreatic islets (Fig. 3*M–P*).

FGF21 inhibits hepatic lipogenic, adipogenic, and glucose production pathways. Hepatic lipid metabolism was studied to understand the molecular mechanisms underlying FGF21 reduction of hepatic steatosis. We found that expression levels of multiple genes involved in fatty acid oxidation or uncoupling were upregulated in mice fed high-fat diet compared with expression levels in mice fed standard diet (supplementary Fig. 1*B*, available in an online appendix at http://dx.doi.org/10.2337/db08-0392), indicating an increased requirement for fatty acid oxidation during high-fat diet feeding. Treatment with FGF21 did not further increase the expression of fatty acid oxidative genes (supplementary Fig. 1*B*). In contrast, FGF21 dose dependently reduced the amount of the nuclear form of SREBP-1 without changing the amount of the membrane precursor or its mRNA (Fig. 4*A* and *C*). A cluster of SREBP-1 target genes involved in hepatic glycolysis and de novo fatty acid and triglyceride biosynthesis were also downregulated after FGF21 treatment (Fig. 4*C*). The enzyme levels of ACC and FAS were also reduced (Fig. 4*B*). The expression of PPARγ and its target genes adipocyte fatty acid binding protein-2 (aP2) and CD36 were elevated in the livers of DIO mice and reduced after FGF21 treatment (Fig. 4*B* and *D*). On the other hand, the PPARγ ligand rosiglitazone dramatically increased hepatic

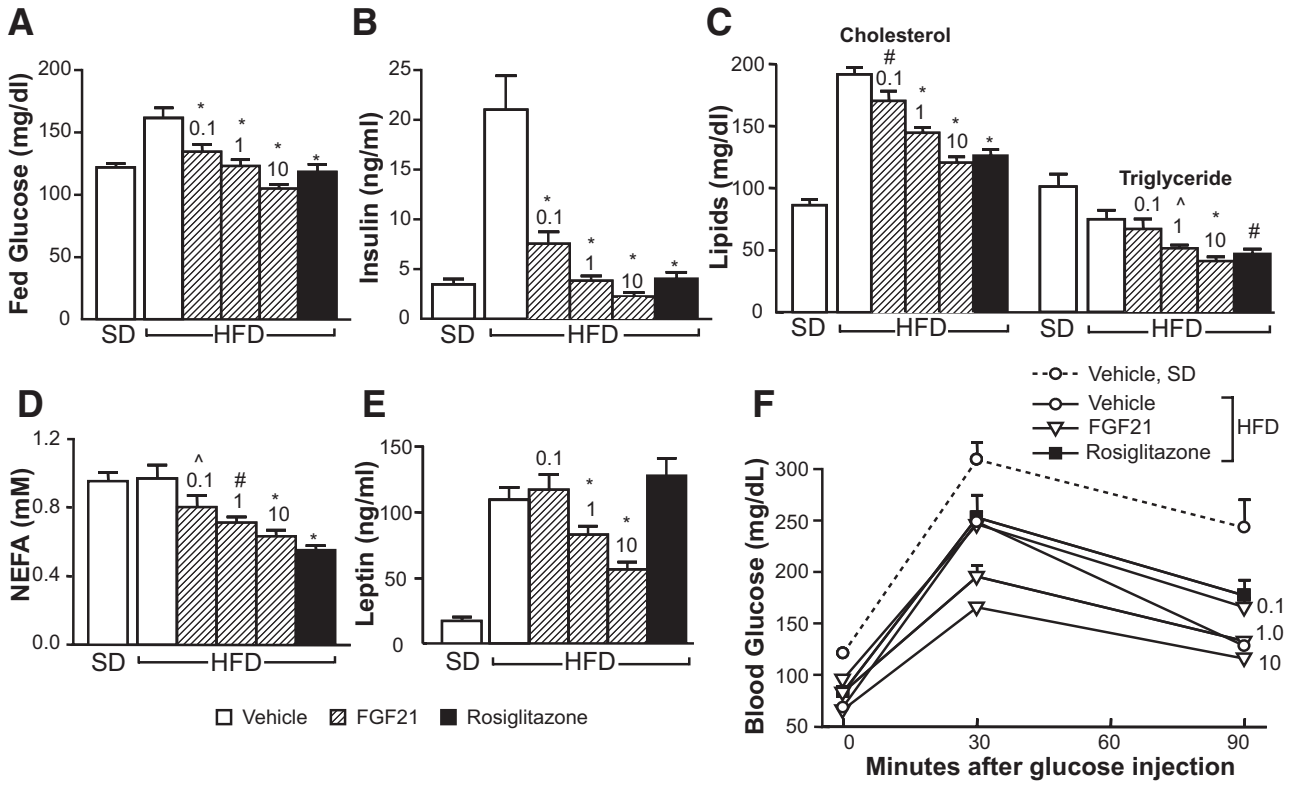

FIG. 2. Recombinant FGF21 reduces plasma glucose, insulin, and lipid levels and improves glucose tolerance in DIO mice. Mice were treated with vehicle or recombinant murine FGF21 intraperitonally at doses of 0 (vehicle), 0.1, 1, or 10 mg · kg^{-1} · day^{-1} divided into two daily injections (8:00 A.M. and 4:00 P.M.). Mice were fed ad libitum, and blood was collected 1 h after the morning injection on study day 24. *A*: Blood glucose. *B*: Plasma insulin. *C*: Plasma cholesterol and triglyceride levels. *D*: Plasma nonesterified free fatty acid (NFFA) levels. *E*: Plasma leptin. *F*: GTT was initiated 1 h after the morning injection on study day 30. Fasted mice were intraperitonally injected with 2 mg/kg glucose solution, and blood glucose was measured at 0 min (before glucose injection) and at 30 and 90 min (after glucose injection). Vehicle (open circles or open bars); FGF21 (open triangles or striped bars; 0.1, 1, and 10 denote FGF21 doses in mg · kg^{-1} · day^{-1}); rosiglitazone (black squares or black bars). All data are means ± SE, n = 10 per group, $\wedge P < 0.05$; #$P < 0.01$; *$P < 0.001$ vs. vehicle-treated high-fat diet mice. NEFA, nonesterified fatty acid.

aP2 and CD36 expression (Fig. 4*D*). FGF21 also reduced the mRNA expression levels of glucose-6-phosphatase without affecting PEPCK (Fig. 4*E*), suggesting that FGF21 may inhibit glucose release from glycogenolysis.

Recombinant FGF21 increases energy expenditure and physical activity. Treatment with FGF21 reduced body weight without altering food intake in DIO mice, suggesting alterations in energy metabolism. We per-

TABLE 1
Liver and plasma metabolic parameters in mice fed standard diet or high-fat diet and treated with vehicle, FGF21, and rosiglitazone

	Standard diet	High-fat diet				
			FGF21			
Parameters	Vehicle	Vehicle	0.1 mg/kg	1 mg/kg	10 mg/kg	Rosiglitazone
Body weight (g)*	32.6 ± 1.2†	49.1 ± 0.8	51.2 ± 0.9	46.1 ± 1.1	38.0 ± 1.0†	56.2 ± 2.1†
Liver weight (g)*	1.5 ± 0.1†	2.5 ± 0.2	1.9 ± 0.2	1.5 ± 0.11†	1.2 ± 0.5†	2.9 ± 0.14
Liver triglyceride (mg/g)*	10 ± 2.5†	154 ± 13.4	103 ± 27.5‡	47 ± 2.5†	23 ± 1.5†	212 ± 6.6§
Liver cholesterol (mg/g)*	1.6 ± 0.1†	6.4 ± 1.0	4.1 ± 1.0‡	1.6 ± 0.1†	1.7 ± 0.1†	6.7 ± 0.5
Gastrocnemic muscle weight (g)*	0.36 ± 0.01	0.38 ± 0.02	0.39 ± 0.01	0.37 ± 0.01	0.35 ± 0.01	0.37 ± 0.01
Muscle triglyceride (mg/g)*	16 ± 1.7†	65 ± 6.6	64 ± 11	60 ± 7.5	37 ± 4.6‡	90 ± 15
Muscle cholesterol (mg/g)*	1.1 ± 0.06	1.7 ± 0.4	1.7 ± 0.4	1.3 ± 0.07	1.1 ± 0.05	2.1 ± 0.4
Plasma ALT (units/l)¶	25 ± 2.6†	248 ± 69.7	82 ± 16.6§	44 ± 4.5†	30 ± 5.4†	142 ± 32.7‡
Plasma AST (units/l)¶	49 ± 4.6†	205 ± 48	102 ± 17§	81 ± 6.5†	69 ± 7.6†	128 ± 17.6‡
Plasma ALP (units/l)¶	54 ± 1.5‡	71 ± 8.7	45 ± 3.1§	33 ± 3.8†	30 ± 2†	81 ± 7.2
Plasma glucagon (pg/ml)¶	305 ± 88	280 ± 63	379 ± 118	204 ± 33	236 ± 35	250 ± 48
Plasma β-hydroxyburate (nmol/l)*	0.62 ± 0.07§	0.85 ± 0.05	0.84 ± 0.04	0.58 ± 0.06§	0.61 ± 0.05§	0.56 ± 0.05§

Data are means ± SE. DIO mice were treated with recombinant murine FGF21 intraperitoneally at doses of 0 (vehicle), 0.1, 1, or 10 mg · kg^{-1} · day^{-1}. An additional group of DIO mice was treated with rosiglitazone formulated in the high-fat diet to provide a dose of ~4 mg · kg^{-1} · day^{-1}. Mice on normal standard diet were included as controls and were injected intraperitoneally with vehicle. *,¶Measurements that were conducted on day 42 (n = 5/group) or day 24 (n = 10/group) after the initiation of the treatments, respectively. ‡$P < 0.05$, §$P < 0.01$, †$P < 0.001$ vs. vehicle-treated DIO mice.

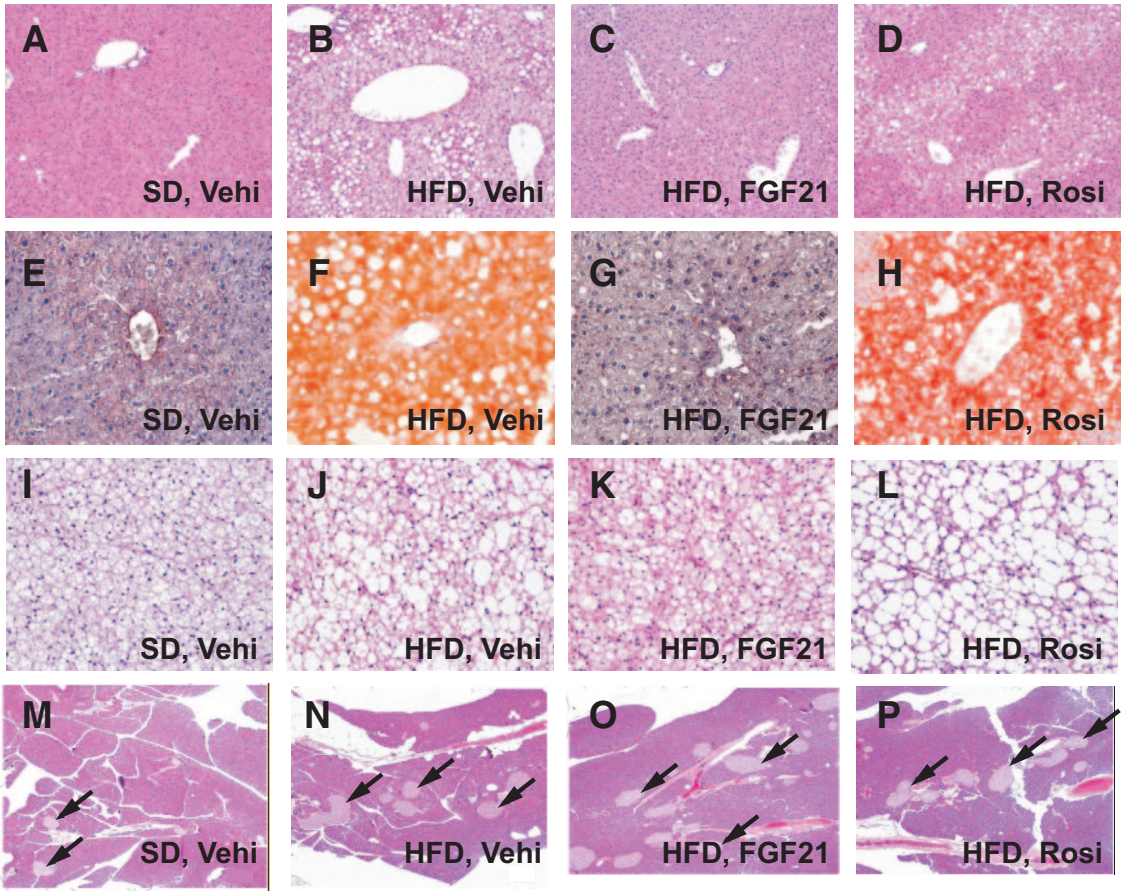

FIG. 3. Tissue histological analysis. Tissue sections were prepared at the end of the 6-week treatment period from mice fed standard diet and treated with vehicle (*A*, *E*, *I*, and *M*) or fed high-fat diet and treated with vehicle (Vehi.; *B*, *F*, *J*, and *N*), FGF21 (10 mg · kg^{-1} · day^{-1}; *C*, *G*, *K*, and *O*), or rosiglitazone (~4 mg · kg^{-1} · day^{-1}; *D*, *H*, *L*, and *P*). H-E (*A–D*) and oil-red-O (*E–H*) staining of liver sections shows reversal of vacuolation and lipid accumulation in FGF21-treated DIO mice. *I–L*: H-E staining of brown adipose tissue reveals the reduction of large lipid vacuoles in FGF21-treated DIO mice. *M–P*: H-E staining of pancreatic sections shows the neutral effects of FGF21 on islet morphology (indicated by arrows). (Please see http://dx.doi.org/10.2337/db08-0392 for a high-quality digital representation of this figure.)

formed indirect calorimetry to assess energy expenditure and substrate oxidation (respiratory quotient) by measuring O_2 consumption and CO_2 production. Figure 5*A* shows a biphasic circadian rhythm of O_2 consumption typical for the nocturnal habits of a rodent. We were able to detect a statistically significant increase in O_2 consumption in DIO mice treated with FGF21 on day 2 (Fig. 5*A*, arrow), and this effect became progressively more evident as the treatment continued. Associated with the increase in O_2 consumption (Fig. 5*A* and *B*), CO_2 production (Fig. 5*C*) and physical activity (Fig. 5*D*) were also increased in mice treated with FGF21. Energy expenditure was also increased in FGF21-treated mice (Fig. 5*E*). The respiratory quotient was not different between FGF21- and vehicle-treated mice (Fig. 5*F*), suggesting that FGF21 does not alter fuel selection between fatty acids and carbohydrate.

Recombinant FGF21 improves whole-body insulin sensitivity and glucose metabolism. We performed a 2-h hyperinsulinemic-euglycemic clamp combined with intravenous administration of [3-^{3}H]glucose and [1-^{14}C]2-deoxyglucose in mice fed standard diet or high-fat diet for 15 weeks and treated with FGF21 or vehicle during the last 3 weeks of diet period. The basal (overnight-fasted) and clamp glucose and insulin levels are shown in supplementary Table 1, available in the online appendix. Treatment with 10 mg · kg^{-1} · day^{-1} FGF21 restored the glucose infusion rate to normal in DIO mice and further enhanced insulin responsiveness in mice fed standard diet (Fig. 6*A*). The improved insulin sensitivity was associated with reduced basal (Fig. 6*B*) and clamp hepatic glucose production (HGP) (Fig. 6*C*) and increased whole-body glucose turnover in FGF21-treated mice (Fig. 6*D–F*). The increased glucose metabolism was reflected in significantly elevated whole-body glycogen plus lipid synthesis (Fig. 6*F*) and modestly elevated whole-body glycolysis (Fig. 6*E*).

Tissue-specific glucose uptake was measured using 2-deoxyglucose during clamps. FGF21 treatment (10 mg · kg^{-1} · day^{-1}) restored glucose uptake in skeletal muscle and heart to normal levels in DIO mice (Fig. 7*A* and *D*). Insulin-stimulated glucose uptake in white and brown adipose tissue was enhanced in both standard diet– and high-fat diet–fed mice after FGF21 treatment (Fig. 7*B* and *C*), suggesting that these tissues were highly responsive to FGF21. A dose level of 0.1 mg · kg^{-1} · day^{-1} FGF21 increased glucose infusion rate (Fig. 6*A*), suppressed HGP (Fig. 6*C*), and increased peripheral glucose uptake (Fig. 7*A*, *C*, and *D*) during clamp without reduction of body weight (supplementary Table 1).

DISCUSSION

We administered recombinant murine FGF21 to DIO mice, and we report that FGF21 corrects multiple metabolic disorders in this model. We demonstrate that FGF21 reduces body weight, reverses hepatic steatosis, increases

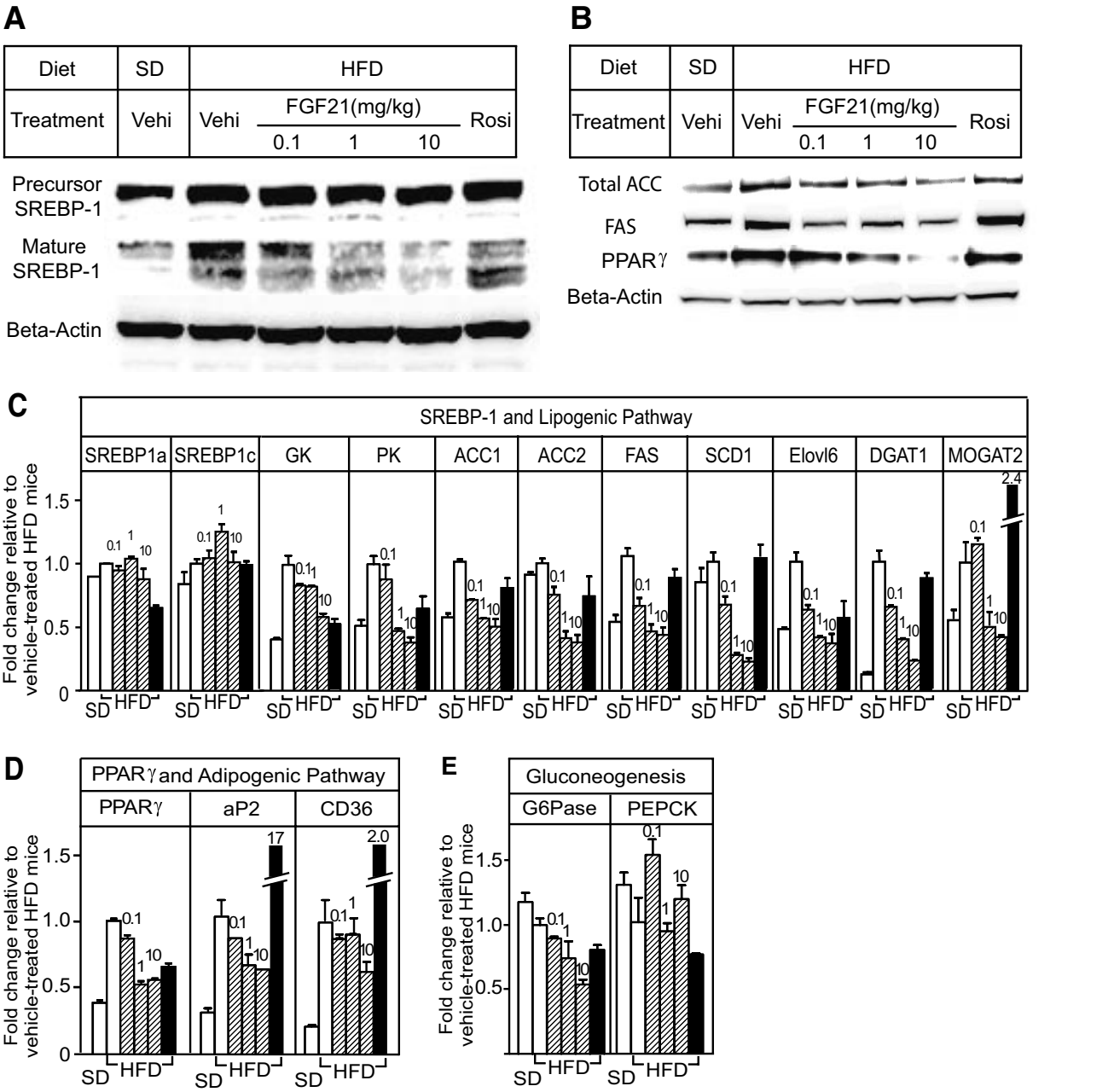

FIG. 4. Hepatic protein and gene expression analysis. Total protein and RNA were extracted from frozen liver samples of mice fed standard diet and administered vehicle (open bars, SD), fed high-fat diet and administered vehicle (open bars, HFD), FGF21 (striped bars; 0.1, 1, and 10 mg · kg^{-1} · day^{-1} doses), or rosiglitazone (black bars; ~4 mg · kg^{-1} · day^{-1}) for 6 weeks. Western analyses and RT-PCRs were conducted on pooled protein and RNA extracts (n = 5 per group). *A*: FGF21 reduced the amount of mature SREBP-1 without changing its precursor content in liver. Vehi, vehicle; Rosi, rosiglitazone. *B*: FGF21 reduced protein expression levels of total ACC, FAS, and PPARγ in liver. *C*: FGF21 reduced mRNAs encoding enzymes involved in hepatic lipogenesis without changing SREBP-1 mRNA expression. GK, glucokinase; PK, pyruvate kinase; SCD1, stearoyl-CoA desaturase 1; Elovl6, long-chain fatty acid elongase 6; DGAT1 and MOGAT2, diacylgycerol and monoacyglycerol acyltransferases. *D*: FGF21 reduced mRNA expression of PPARγ and its target genes, aP2 and CD36, in liver. *E*: FGF21 reduced glucose-6-phosphatase (G6Pase) mRNA expression.

whole-body energy expenditure, and improves hepatic and peripheral insulin sensitivity.

A moderate weight loss effect of recombinant FGF21 was observed in previous studies conducted in primates (8) but not in obese rodents such as *ob/ob* mice or ZDF rats (5). In contrast, we show that administration of recombinant FGF21 led to dramatic body weight loss in DIO mice without reducing food intake or causing apparent discomfort. Our data are in agreement with phenotypes of FGF21 transgenic mice, which are lean and resistant to high-fat diet–induced obesity (5,9). The variable body weight reduction results among recombinant protein studies may lie in the differences in FGF21 administration frequency, dose levels, or animal models. We have found that FGF21-induced body weight reduction is dose related. The dose required to reduce adiposity (1 and 10 mg · kg^{-1} · day^{-1}) is higher that that required to improve insulin sensitivity and glucose metabolism (0.1 mg · kg^{-1} · day^{-1}). Nevertheless, FGF21 reduction of body weight appears not to be leptin dependent because the same FGF21 doses resulted in similar body weight reduction in *ob/ob* mice (data not shown).

The antiobesity effect of FGF21 is to some extent mediated by regulating energy metabolism. We show that

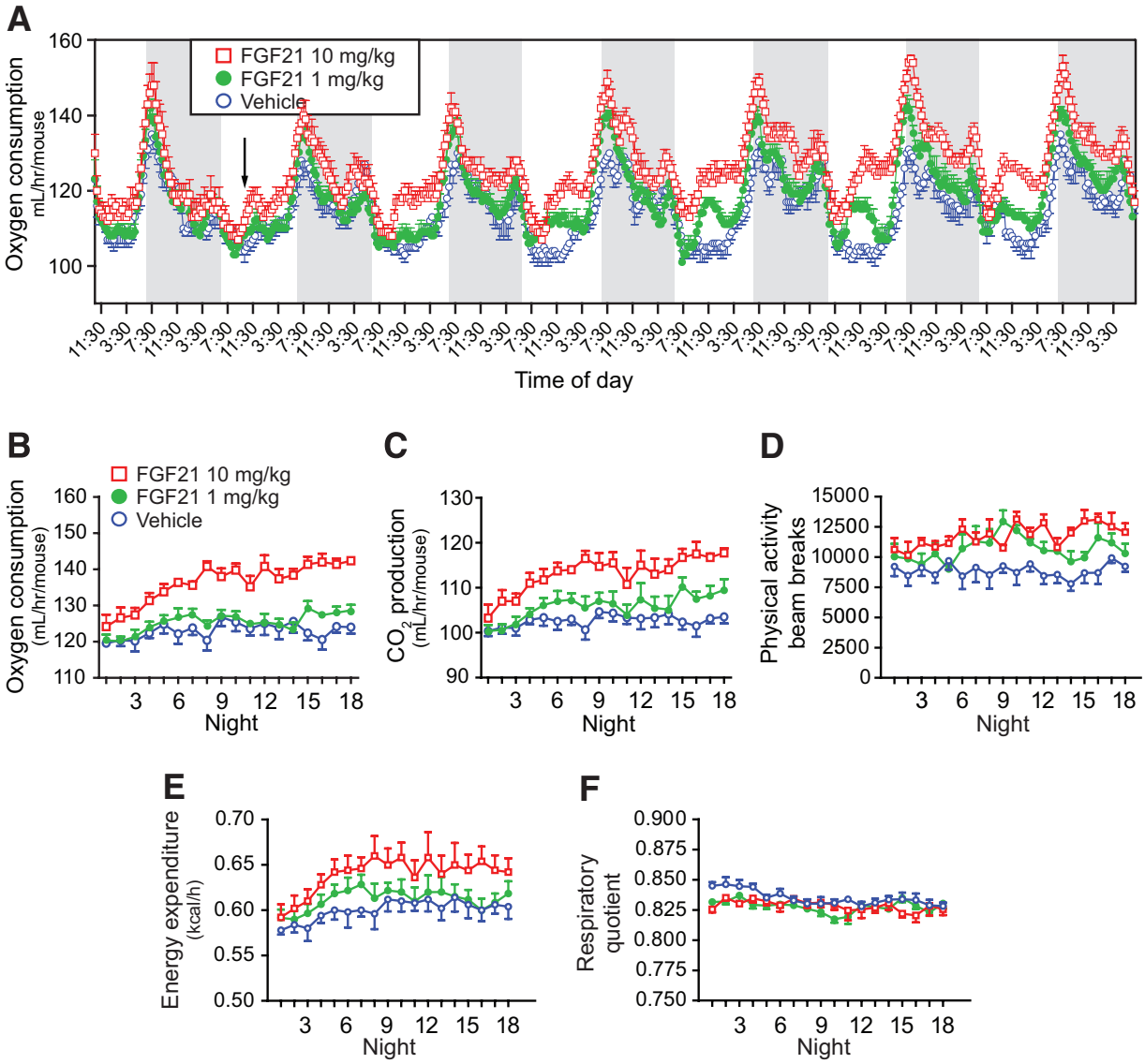

FIG. 5. Recombinant FGF21 increases energy expenditure and physical activity in DIO mice. Indirect calorimetry was conducted continuously for 19 days. DIO mice were injected intraperitonally with FGF21 at doses of 10 mg · kg^{-1} · day^{-1} (red open squares, n = 5) and 1 mg · kg^{-1} · day^{-1} (green filled circles, n = 6) or vehicle (blue open circles, n = 5). *A*: FGF21 treatment elevated O_2 consumption. Measurements were collected every 20 min, and each data point represents a rolling average of six time points. Dark periods (6:30 P.M. to 6:30 A.M.) are shown by a shaded gray box. Arrow marks first statistically significant difference between FGF21 10 mg · kg^{-1} · day^{-1} and vehicle. All data are means of multiple mice ± SE. Data shown are the first 7 days of the treatment. O_2 consumption (*B*), CO_2 production (*C*), physical activity (*D*), energy expenditure (*E*), and respiratory quotient (*F*) in the dark periods were monitored for the entire 19 days. Data in *B–F* represent the average from the whole dark period. All means are shown with SE.

FGF21 stimulates whole-body energy expenditure and increases metabolic rate and physical activity. Consistent with the increased metabolic rate, administration of FGF21 altered body composition, with a dramatic reduction in body fat mass and a small reduction in lean mass. FGF21 appears to not change the preference in fatty acid and carbohydrate utilization suggested by the unaltered respiratory quotient. The reduced physical activity has been shown to be a causative factor that accounts for 50% of body weight gain in DIO rodents (20). FGF21 significantly increased locomotor activity levels, indicating the importance of activity in FGF21-induced weight loss. This observation is intriguing because FGF21 could be used as an antiobesity agent, given that reduced spontaneous physical activity and the resulting reduction of nonexercise activity thermogenesis are critical factors contributing to the development of human obesity (21). Recently reported data suggest that FGF21 administration increased body temperature in DIO mice (22). Although we did not measure body temperature, mice treated with FGF21 had reduced lipid accumulation (Fig. 3*K*) and increased levels of UCP-1 and -2 mRNA expression in brown adipocytes (supplementary Fig. 1*A*). Therefore, brown adipose tissue adaptive thermogenesis may have also contributed to the enhanced whole-body energy expenditure.

Interestingly, our findings appear to conflict with a previous publication that indicated that FGF21 stimulates torpor, reduces energy expenditure, and decreases physical activity (9). A significant difference between the two studies was that our energy metabolism study was conducted in mice with free access to food, whereas the other study was conducted in 24-h–fasted mice. The seemingly divergent results suggest that the effect of FGF21 on energy homeostasis may be subject to a feedback regulation of nutritional and feeding status. The brain has been

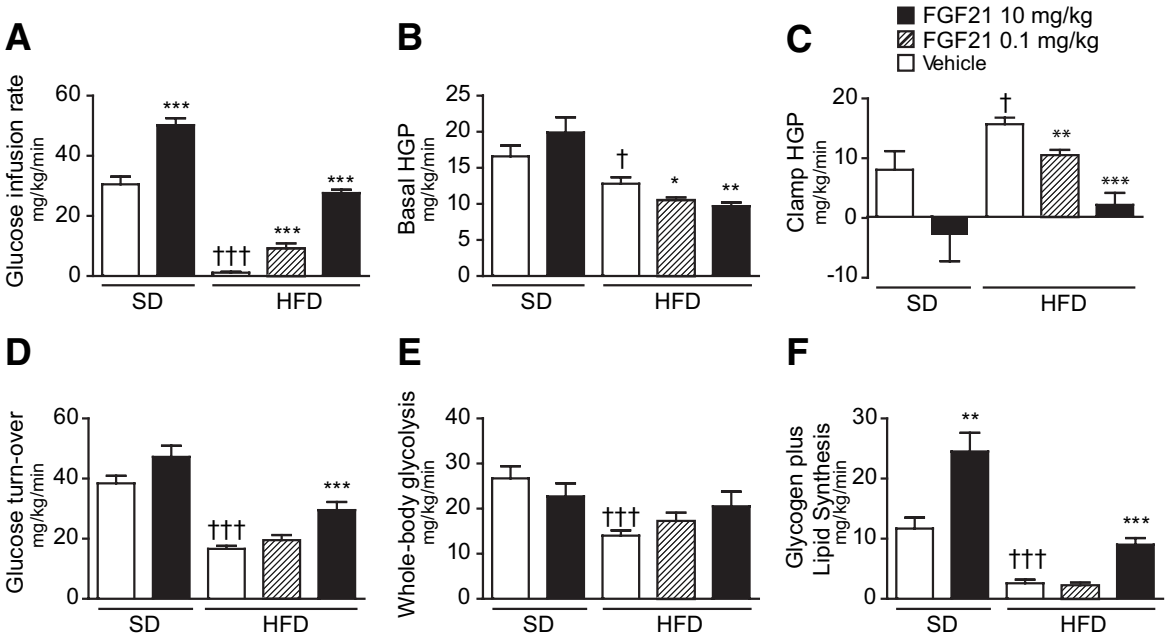

FIG. 6. Recombinant FGF21 improves whole-body glucose metabolism in both lean and DIO mice. Hyperinsulinemic-euglycemic clamps were conducted on standard diet– or high-fat diet–fed mice treated with vehicle (open bars), 0.1 (striped bars), or 10 (black bars) mg · kg^{-1} · day^{-1} FGF21 for 21 days. *A*: Steady-state glucose infusion rate, obtained from averaged rates of 90–120 min of hyperinsulinemic-euglycemic clamps. *B*: Basal rates of HGP. *C*: Insulin-stimulated rates of HGP during clamps. *D*: Insulin-stimulated whole-body glucose turnover. *E*: Whole-body glycolysis. *F*: whole-body glycogen plus lipid synthesis. All data are means ± SE; standard diet–vehicle (n = 10); standard diet–FGF21 treated (n = 8); high-fat diet–all groups (n = 12). *P < 0.05, **P < 0.01, ***P < 0.001 vs. vehicle-treated (diet-matched) mice, †P< 0.01, †††P < 0.0001 vs. standard diet–vehicle–treated mice.

recognized as a control center that integrates hormonal and nutritional signals from the periphery and transmits the control over feeding, energy expenditure, and physical activity (23). Future studies will be needed to understand whether FGF21 effects on energy metabolism involve a central nervous system-associated mechanism.

FGF21 has previously been shown to lower blood glucose levels in several diabetic rodent and monkey models (5,8). Here, we show that FGF21 simultaneously reduced plasma glucose and insulin levels in DIO mice without causing fasting hypoglycemia, which is consistent with what has been observed in other models (5). We further demonstrate that the glucose-lowering effect of FGF21 is linked with improved insulin sensitivity in suppression of HGP and stimulation of peripheral glucose uptake. FGF21 appears to play major roles in both insulin

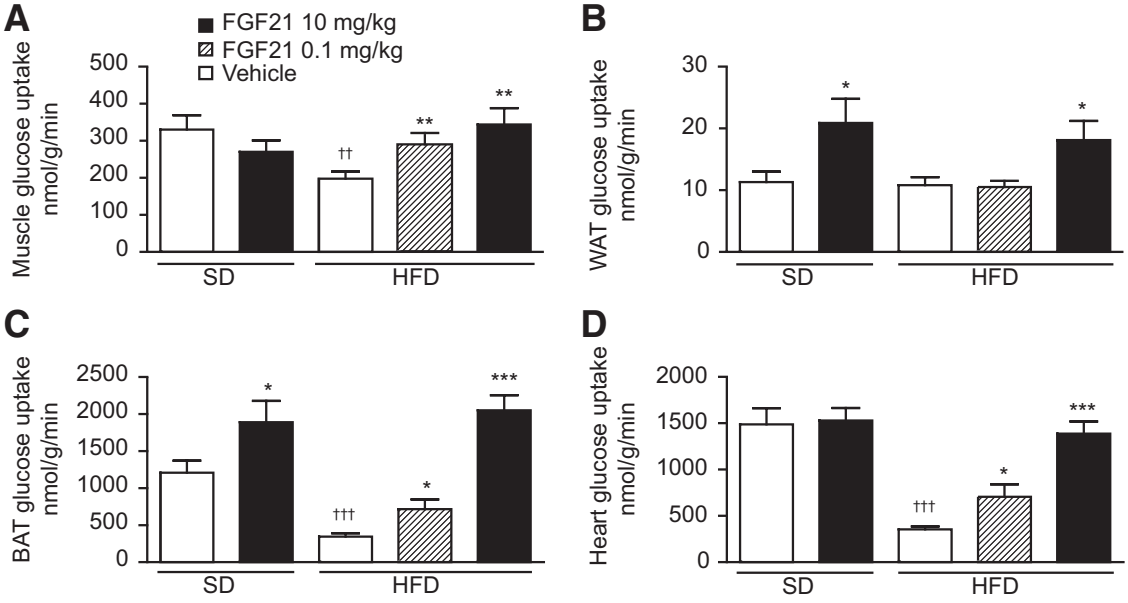

FIG. 7. Recombinant FGF21 improves tissue-specific glucose uptake in lean and DIO mice. Insulin-stimulated glucose uptake in individual organs during clamps was assessed using 2-[^{14}C]deoxyglucose uptake assay on standard diet or high-fat diet mice treated with vehicle (open bars), 0.1 (striped bars), or 10 (black bars) mg · kg^{-1} · day^{-1} FGF21 for 3 weeks. Insulin-stimulated rates of glucose uptake are shown for skeletal muscle (*A*), white adipose tissue (WAT) (*B*), brown adipose tissue (BAT) (*C*), and heart (*D*). All data are means ± SE; standard diet–vehicle (n = 10); standard diet–FGF21 treated (n = 8); high-fat diet–all groups (n = 12). *P < 0.05, **P < 0.01, ***P < 0.001 vs. vehicle-treated (diet-matched) mice, ††P < 0.05, †††P < 0.0001 vs. standard diet–vehicle–treated mice.

sensitivity and energy metabolism. In our pharmacology studies, we determined that a dose level of 0.1 $mg \cdot kg^{-1} \cdot day^{-1}$ FGF21 did not reduce body weight and adiposity. This dose was therefore specifically chosen for the hyperinsulinemic-euglycemic clamp study on DIO mice so that insulin sensitivity could be studied independently of body weight and adiposity. We found that FGF21, at this dose level, increased hepatic and peripheral insulin sensitivity, reduced plasma levels of glucose and lipids, and restored glucose tolerance. Therefore, FGF21-induced insulin sensitivity is not secondary to body weight reduction. Although understandably, reduced obesity further enhanced insulin sensitivity as demonstrated with the high dose (10 $mg \cdot kg^{-1} \cdot day^{-1}$) of FGF21.

The insulin-sensitizing effect of FGF21 was also observed in *ob/ob* mice, a model of more severe hyperglycemia than the DIO mouse model (24). In that study, FGF21 restored insulin-mediated suppression of hepatic glucose output and increased cardiac glucose uptake after 7 days of treatment. Our hyperinsulinemic-euglycemic clamp study was conducted in mice after 3 weeks of chronic FGF21 treatment, and we observed improved insulin sensitivity in multiple insulin-responsive tissues, including liver, adipose tissue, skeletal muscle, and heart. FGF21 action requires a coreceptor, β-klotho (11), which is abundantly expressed in adipose tissues, readily detectable in liver, and insignificant in skeletal muscle and perhaps the heart (supplementary Fig. 1*C*; 13). Based on β-klotho expression, FGF21 may act directly on liver and adipose tissue and indirectly on skeletal muscle and heart. This hypothesis is corroborated by the observation that FGF21 improved hepatic and adipose tissue insulin sensitivity irrespective of diet or disease state. In contrast, it restored skeletal muscle and heart glucose uptake activity only in mice fed high-fat diet and not standard diet. The direct FGF21 action on liver and adipose tissue is possibly mediated through induction of signaling transduction and alteration in gene expression. It has been reported that FGF21 induces FGF signaling and stimulates GLUT1 expression and glucose uptake in adipose tissue (5,25). We have also observed reduced hepatic glucose-6-phosphatase and lipogenic gene expression and ameliorated hepatosteatosis after FGF21 treatment. Such metabolic changes would be expected to improve hepatic insulin sensitivity and enhance insulin-mediated suppression of HGP. The restored insulin sensitivity in skeletal muscle and heart of FGF21-treated DIO mice could be a secondary consequence of improved hepatic and adipose tissue functions. As hepatosteatosis and adiposity were ameliorated in DIO mice treated with FGF21, skeletal muscle triglyceride contents were also reduced (Table 1). This reduction of muscle fat accumulation is known to restore muscle function and muscle insulin sensitivity (26).

FGF21 treatment resulted in striking improvement of high-fat diet–induced hepatic steatosis. FGF21 has been suggested to increase hepatic ketogenesis by mobilizing adipocyte fatty acids to liver for oxidation (9). Surprisingly, we were unable to find evidence of increased hepatic ketogenesis or adipose tissue lipolysis. The plasma β-hydroxybutyrate and free fatty acid levels were dose dependently reduced in FGF21-treated DIO mice, which argues against an increase in ketogenesis and lipolysis. It is possible that our observed reduction in ketone bodies and free fatty acid levels reflects a long-term effect of FGF21 treatment after improved hepatic and adipose tissue insulin sensitivity (27). Nevertheless, a recent human study indicated a lack of correlation between plasma FGF21 concentration and ketone bodies, suggesting a weak cause-effect relationship between FGF21 and ketogenesis, at least in humans (28).

Here, we provide evidence that FGF21 reduces hepatic steatosis by inhibiting nuclear SREBP-1 maturation and therefore leads to reduced lipogenic gene expression and possibly the rate of de novo fatty acid and triglyceride synthesis. SREBP-1 is a transcription factor critical for lipogenesis and is involved in the induction of hepatic steatosis in several animal models (29,30). SREBP-1 is synthesized as a membrane precursor form that requires proteolytic cleavage to release its active NH_2-terminal transcription factor to translocate to the nucleus (31). Treatment with FGF21 reduced the nuclear form of SREBP-1 without affecting the amount of the precursor protein or its mRNA, suggesting that FGF21 may inhibit SREBP-1 proteolytic processing. FGF21 is a signaling molecule acting through receptor-mediated kinase cascades involving extracellular signal–related kinase-1/2 and other typical FGF signaling pathways (5,14). How the FGF21 signaling pathway affects SREBP-1 cleavage and whether the regulation is mediated by SREBP cleavage-activating protein and insulin-induced gene protein complex are subjects for future investigation. Aberrant induction of hepatic PPARγ expression has also been shown to contribute to hepatic steatosis in several insulin-resistant models of obesity (32). In our experiments with DIO mice, the hepatic expression of PPARγ was increased. Rosiglitazone further increased PPARγ activity, as demonstrated by increased expression of aP2 and CD36 and worsened hepatic steatosis. In contrast, administration of FGF21 reduced PPARγ, aP2, and CD36 expression, which may provide an additional mechanism for the observed amelioration of hepatic steatosis.

In summary, our findings provide physiological and molecular evidence that FGF21 reduces body weight, plasma glucose, and lipid levels by regulating energy homeostasis, hepatic glucose and lipid metabolism, and insulin sensitivity.

ACKNOWLEDGMENTS

No potential conflicts of interest relevant to this article were reported.

We thank Narumol Chinookoswong, Jim Busby, Smith Stephen, and Fisher Seth for their technical support. We thank Scott Silbiger for providing editorial support in the preparation of this manuscript and Tom Boone for helpful discussions and support.

REFERENCES

1. Itoh N, Ornitz DM: Evolution of the Fgf and Fgfr gene families. *Trends Genet* 20:563–569, 2004
2. Goetz R, Beenken A, Ibrahimi OA, Kalinina J, Olsen SK, Eliseenkova AV, Xu C, Neubert TA, Zhang F, Linhardt RJ, Yu X, White KE, Inagaki T, Kliewer SA, Yamamoto M, Kurosu H, Ogawa Y, Kuro-o M, Lanske B, Razzaque MS, Mohammadi M: Molecular insights into the klotho-dependent, endocrine mode of action of fibroblast growth factor 19 subfamily members. *Mol Cell Biol* 27:3417–3428, 2007
3. Fu L, John LM, Adams SH, Yu XX, Tomlinson E, Renz M, Williams PM, Soriano R, Corpuz R, Moffat B, Vandlen R, Simmons L, Foster J, Stephan JP, Tsai SP, Stewart TA: Fibroblast growth factor 19 increases metabolic rate and reverses dietary and leptin-deficient diabetes. *Endocrinology* 145:2594–2603, 2004
4. Inagaki T, Choi M, Moschetta A, Peng L, Cummins CL, McDonald JG, Luo G, Jones SA, Goodwin B, Richardson JA, Gerard RD, Repa JJ, Mangelsdorf

DJ, Kliewer SA: Fibroblast growth factor 15 functions as an enterohepatic signal to regulate bile acid homeostasis. *Cell Metab* 2:217–225, 2005
5. Kharitonenkov A, Shiyanova TL, Koester A, Ford AM, Micanovic R, Galbreath EJ, Sandusky GE, Hammond LJ, Moyers JS, Owens RA, Gromada J, Brozinick JT, Hawkins ED, Wroblewski VJ, Li DS, Mehrbod F, Jaskunas SR, Shanafelt AB: FGF-21 as a novel metabolic regulator. *J Clin Invest* 115:1627–1635, 2005
6. Yu X, White KE: FGF23 and disorders of phosphate homeostasis. *Cytokine Growth Factor Rev* 16:221–232, 2005
7. Nishimura T, Nakatake Y, Konishi M, Itoh N: Identification of a novel FGF, FGF-21, preferentially expressed in the liver. *Biochim Biophys Acta* 1492:203–206, 2000
8. Kharitonenkov A, Wroblewski VJ, Koester A, Chen YF, Clutinger CK, Tigno XT, Hansen BC, Shanafelt AB, Etgen GJ: The metabolic state of diabetic monkeys is regulated by fibroblast growth factor-21. *Endocrinology* 148: 774–781, 2007
9. Inagaki T, Dutchak P, Zhao G, Ding X, Gautron L, Parameswara V, Li Y, Goetz R, Mohammadi M, Esser V, Elmquist JK, Gerard RD, Burgess SC, Hammer RE, Mangelsdorf DJ, Kliewer SA: Endocrine regulation of the fasting response by PPARalpha-mediated induction of fibroblast growth factor 21. *Cell Metab* 5:415–425, 2007
10. Kurosu H, Choi M, Ogawa Y, Dickson AS, Goetz R, Eliseenkova AV, Mohammadi M, Rosenblatt KP, Kliewer SA, Kuro-o M: Tissue-specific expression of betaKlotho and fibroblast growth factor (FGF) receptor isoforms determines metabolic activity of FGF19 and FGF21. *J Biol Chem* 282:26687–26695, 2007
11. Ogawa Y, Kurosu H, Yamamoto M, Nandi A, Rosenblatt KP, Goetz R, Eliseenkova AV, Mohammadi M, Kuro-o M: BetaKlotho is required for metabolic activity of fibroblast growth factor 21. *Proc Natl Acad Sci U S A* 104:7432–7437, 2007
12. Kharitonenkov A, Dunbar JD, Bina HA, Bright S, Moyers JS, Zhang C, Ding L, Micanovic R, Mehrbod SF, Knierman MD, Hale JE, Coskun T, Shanafelt AB: FGF-21/FGF-21 receptor interaction and activation is determined by betaKlotho. *J Cell Physiol* 215:1–7, 2008
13. Ito S, Kinoshita S, Shiraishi N, Nakagawa S, Sekine S, Fujimori T, Nabeshima YI: Molecular cloning and expression analyses of mouse betaklotho, which encodes a novel Klotho family protein. *Mech Dev* 98:115–119, 2000
14. Wente W, Efanov AM, Brenner M, Kharitonenkov A, Koster A, Sandusky GE, Sewing S, Treinies I, Zitzer H, Gromada J: Fibroblast growth factor-21 improves pancreatic beta-cell function and survival by activation of extracellular signal-regulated kinase 1/2 and Akt signaling pathways. *Diabetes* 55:2470–2478, 2006
15. Badman MK, Pissios P, Kennedy AR, Koukos G, Flier JS, Maratos-Flier E: Hepatic fibroblast growth factor 21 is regulated by PPARalpha and is a key mediator of hepatic lipid metabolism in ketotic states. *Cell Metab* 5:426–437, 2007
16. Folch J, Lees M, Sloane Stanley GH: A simple method for the isolation and purification of total lipids from animal tissues. *J Biol Chem* 226:497–509, 1957
17. Yokode M, Hammer RE, Ishibashi S, Brown MS, Goldstein JL: Diet-induced hypercholesterolemia in mice: prevention by overexpression of LDL receptors. *Science* 250:1273–1275, 1990
18. Vavvas D, Apazidis A, Saha AK, Gamble J, Patel A, Kemp BE, Witters LA, Ruderman NB: Contraction-induced changes in acetyl-CoA carboxylase and 5′-AMP-activated kinase in skeletal muscle. *J Biol Chem* 272:13255–13261, 1997
19. Kim HJ, Higashimori T, Park SY, Choi H, Dong J, Kim YJ, Noh HL, Cho YR, Cline G, Kim YB, Kim JK: Differential effects of interleukin-6 and -10 on skeletal muscle and liver insulin action in vivo. *Diabetes* 53:1060–1067, 2004
20. Bjursell M, Gerdin AK, Lelliott CJ, Egecioglu E, Elmgren A, Tornell J, Oscarsson J, Bohlooly YM: Acutely reduced locomotor activity is a major contributor to Western diet-induced obesity in mice. *Am J Physiol Endocrinol Metab* 294:E251–E260, 2008
21. Levine JA, Eberhardt NL, Jensen MD: Role of nonexercise activity thermogenesis in resistance to fat gain in humans. *Science* 283:212–214, 1999
22. Coskun T, Bina HA, Schneider MA, Dunbar JD, Hu CC, Chen Y, Moller DE, Kharitonenkov A: FGF21 corrects obesity in mice. *Endocrinology*. In press
23. Spiegelman BM, Flier JS: Obesity and the regulation of energy balance. *Cell* 104:531–543, 2001
24. Berglund ED, Li CY, Lynes SE, Bina HA, Michael MD, Kharitonenkov A, Wasserman DH: Chronic FGF-21 treatment improves insulin sensitivity in *ob/ob* mice (Abstract 187-OR). *68th Scientific Meeting of American Diabetes Association, San Francisco, CA, June 6–10, 2008*
25. Moyers JS, Shiyanova TL, Mehrbod F, Dunbar JD, Noblitt TW, Otto KA, Reifel-Miller A, Kharitonenkov A: Molecular determinants of FGF-21 activity-synergy and cross-talk with PPARgamma signaling. *J Cell Physiol* 210:1–6, 2007
26. Pan DA, Lillioja S, Kriketos AD, Milner MR, Baur LA, Bogardus C, Jenkins AB, Storlien LH: Skeletal muscle triglyceride levels are inversely related to insulin action. *Diabetes* 46:983–988, 1997
27. Arner P, Pettersson A, Mitchell PJ, Dunbar JD, Kharitonenkov A, Ryden M: FGF21 attenuates lipolysis in human adipocytes: a possible link to improved insulin sensitivity. *FEBS Lett* 582:1725–1730, 2008
28. Galman C, Lundasen T, Kharitonenkov A, Bina HA, Eriksson M, Hafstrom I, Dahlin M, Amark P, Angelin B, Rudling M: The circulating metabolic regulator FGF21 is induced by prolonged fasting and PPARalpha activation in man. *Cell Metab* 8:169–174, 2008
29. Shimano H, Horton JD, Hammer RE, Shimomura I, Brown MS, Goldstein JL: Overproduction of cholesterol and fatty acids causes massive liver enlargement in transgenic mice expressing truncated SREBP-1a. *J Clin Invest* 98:1575–1584, 1996
30. Browning JD, Horton JD: Molecular mediators of hepatic steatosis and liver injury. *J Clin Invest* 114:147–152, 2004
31. Brown MS, Goldstein JL: A proteolytic pathway that controls the cholesterol content of membranes, cells, and blood. *Proc Natl Acad Sci U S A* 96:11041–11048, 1999
32. Zhang YL, Hernandez-Ono A, Siri P, Weisberg S, Conlon D, Graham MJ, Crooke RM, Huang LS, Ginsberg HN: Aberrant hepatic expression of PPARgamma2 stimulates hepatic lipogenesis in a mouse model of obesity, insulin resistance, dyslipidemia, and hepatic steatosis. *J Biol Chem* 281:37603–37615, 2006